Pressure Profile Consistency in ASDEX Discharges

O. Gruber and G. Becker, H.S. Bosch, H. Brocken, A. Carlson, A. Eberhagen, G. Dodel[1], H.-U. Fahrbach, G. Fussmann, O. Gehre, J. Gernhardt, G. v.Gierke, E. Glock, G. Haas, W. Herrmann, J. Hofmann, A. Izvozchikov[2], E. Holzhauer[1], K. Hübner[3], G. Janeschitz, F. Karger, M. Kaufmann, O. Klüber, M. Kornherr, K. Lackner, M. Lenoci, G. Lisitano, F. Mast, H.M. Mayer, K. McCormick, D. Meisel, V. Mertens, E.R. Müller, H. Murmann, J. Neuhauser, H. Niedermeyer, A. Pietrzyk[4], W. Poschenrieder, H. Rapp, A. Rudyj, F. Schneider, C. Setzensack, G. Siller, E. Speth, F. Söldner, K. Steinmetz, K.-H. Steuer, N. Tsois[5], S. Ugniewski[6], O. Vollmer, F. Wagner, D. Zasche,

Max-Planck-Institut für Plasmaphysik
EURATOM Association, Garching, FRG

1. Introduction

Ohmically (OH) and additionally heated "L-mode" Tokamak discharges exhibit an electron temperature T_e profile invariance against changes in power deposition profiles and plasma density and are only influenced by the safety factor q_a. This has led to the concept of "profile consistency" where the local transport coefficients are not only a function of local plasma parameters but might also depend on non-local processes adjusting the T_e profiles. At present, there exists no coinvincing model for this profile consistency, first introduced by B. Coppi to describe the current density behaviour and the connected T_e profiles of Ohmic heated plasmas. But if the thermal transport is governed, for instance, by electromagnetic modes, not only the current density should show a canonical profile, but also the pressure (p) gradient profiles. Moreover, these profiles can adjust after changes of the heating deposition much faster than the current density, and any deviation from the canonical profile might then result in an additional heat transport which can be expected to act complementory on ion and electrons.

According to Kadomtsev /1/, a pressure profile consistency arises from the existence of relaxed states with thermal and poloidal field minimized subject to a single (constant current) or two constraints (constant current and helicity of the magnetic field). With such a strong principle the resulting pressure and current density profiles depend on the ratio q_a/q_o only and, depending on the constraint, are finite or zero, respectively, at the plasma boundary r=a. Profiles for both cases approach each other at high q_a/q_o. In this paper we examine the total pressure profile shapes in all phases of ASDEX discharges (OH, L and H mode) and compare them with the T_e profiles.

2. T_e and pressure profiles in OH and L mode discharges

There is no commonly agreed format of the T_e profile normalization showing an invariance for different operating conditions. With increasing order of

[1] University of Stuttgart; [2] Ioffe Institute; [3] University of Heidelberg; [4] University of Washington, Seattle, USA; [5] N.R.C.N.S. "Democritos", Athens, Greece; [6] Inst. for Nuclear Research, Swierk, Poland;

the profile consistency quality, the possibilities proposed are: $T(0)/\langle T\rangle$, $T(r)/T(a/2)$ or $\ln(T(r)/T(a/2))$ and $1/T\cdot dT/dr$. Using the normalizaiton $T(r)/T(a/2)$ ASDEX T_e-profiles coincide within the error bars and discharge to discharge variations outside the q=1 surfaces ($r_{q=1}=a/q_a$) for all OH- and L-mode discharge conditions as is shown in Fig. 1 (Thomson scattering measurements). Data from discharges are used for which transport analyses with the TRANSP code have been carried out including stationary and unstationary discharge phases and the following parameter variations: I_p=300÷440 kA, $\bar{n}_e$=1÷11·$10^{19}m^{-3}$; $P_h \leq 3.8$ MW; strong on- and off-axis heating deposition profiles /2/ and pellet refuelled discharges /3/.
For different q_a-values deviations can be seen at radii $r<r_{q=1}$, but differences exist also in the confinement zone between q=1 and q=2 (which is roughly at $r_{q=2}=a/\sqrt{q_a/2}$). This is more clearly demonstrated in Fig. 2 showing for the same discharges the radial profiles of the upper and lower bounds of the normalized T_e scale length r_{Te} given by the inverse logarithmic derivative $r_{Te}/a = -(T_e/dT_e/dr)/a$. Part of the q_a-dependence is certainly due to the T_e-flattening inside the sawtooth region. At fixed q_a there is a weak T_e profile response to changes in the heating profile yielding broader profiles, i.e. higher r_{Te}, with increasing off-axis heat deposition. The latter is obtained by using a lower energy/nucleon of the injected fast neutrals or an increasing density (beam deposition at larger radii, broader resistivity profile due to higher collisionality and reduced $T_e(0)$).

The total kinetic pressure profiles are obtained by using the TRANSP analyses code. Input data are the $n_e(r,t)$ and $T_e(r,t)$ profiles measured by a 16-spatial channel multi-pulse Thomson scattering system and supplemented by a HCN-laser interferometer and ECE diagnostic (4 channels both), the bolometrically measured profiles of the radiation losses and global parameters like the loop voltage V_L, I_p, $\beta_{p\perp}$ from diamagnetic flux measurements and $\beta_{p_\parallel}+l_i/2$ as deduced from poloidal fields and fluxes. Lacking a measurement of the full ion temperature T_i profiles for all discharges we assume a spatially constant enhancement factor α of about 2 to 3 of the ion heat diffusivity χ_i over the neoclassical value as calculated by Chang and Hinton, checking the resulting T_i profiles for their compatibility with the available neutron production and T_i measurements (passive and active CX diagnostic, Doppler broadening of impurity lines). The calculated kinetic pressures include also the contributions due to the anisotropic fast beam ions (using Monte Carlo calculations for the deposition and slowing-down of the beam particles) and are in good agreement with the magnetically measured ones. Fig. 3 shows the pressure scale length r_p for the discharges of Fig. 1 and 2 exhibiting a somewhat stronger separation of the two q_a data sets, which are not in disagreement with the Kadomtsev p(a)=0 pressure profiles. The influence of the χ_i assumption was estimated by taking α-values between 1 and 5, yielding r_p variations below 10%.

3. H-mode profiles

The invariance of the pressure profiles is even more impressive if we look at their time development during single discharges as is shown for a β-limit discharge in Fig. 4. Fig. 4a demonstrates the strong T_e profile variation at the L/H mode transition where the T_e profile flattens in the

center (higher r_{Te}) and develops shoulders towards the boundary. After reaching β_{max} the T_e profiles flatten even more in the center due to increasing central radiation losses /4, 5/. As also the density profiles form shoulders in the H-mode, the electron pressure (p_e) profiles do the same (see Fig. 4b) but are by far not comparable to the second class of Kadomtsev-profiles with $p(a)\neq 0$ which would have nearly constant r_p for $0.5a<r<a$. Contrary to p_e, the total pressure profile is nearly time independent. In this discharge, the fast ions contribute up to 40 % of the pressure and a comparable amount to the pressure gradient and the ion temperature is well above T_e. The universality of the p profile shape is also demonstrated by comparing H-mode discharges both with H^o and D^o injection, i.e. different deposition profiles (see Fig. 5). The disappearance of the q_a-dependence might be partly caused by the lack of sawteeth.

4. Conclusions

The total pressure profiles of ASDEX discharges exhibit a canonical shape which is preserved also in the H-mode contrary to a changing T_e profile shape. There exists one exception namely the high confinement pellet refuelled discharges revealing a steeper pressure gradient and smaller scale lengths /3/. For instances in a q_a=2.5 ohmic pellet discharge the r_p/a profile is about at the lower bound of the gas fuelled discharges shown in Fig. 3. This might be related to the process limiting the pressure shape yielding a lower bound for the r_p profile which is nearly reached in these pellet discharges. It is interesting that only in the pellet discharges n_i-values below 1 are observed over a large part of the plasma column.

References

/1/ B. Kadomtsev, IAEA-Meeting on Confinement in Tokamaks with Intense Heating, (Nov. 1986), Kyoto

/2/ O. Gruber, et al., Proc. 13th Europ. Conf. on Contr. Fusion and Plasma Heating, Schliersee 1986, Europhys. Conf. Abstr. 10C Part I (1986) 248.

/3/ G. Vlases, O. Gruber, M. Kaufmann, et al., Nucl. Fusion, 27 (1987) 351
M. Kaufmann, et al., to be published in Nucl. Fusion

/4/ O. Gruber, et al., Proc. 11th Conf. on Plasma Phys. and Contr. Nucl. Fus. Research, Kyoto, 1986

/5/ O. Gruber, et al., Proc. 12th Europ. Conf. on Contr. Fusion and Plasma Physics, Budapest 1985. Europhys. Conf. Abstr. 9F, Part I(1985) 18

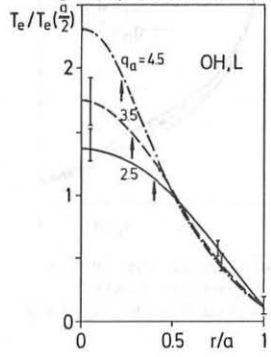

Fig.1: Averaged T_e profiles normalized to $T_e(a/2)$ vs. flux surface radius r in ohmic and L-mode discharges at q_a= 2.5±0.1, and q_a=3.5 ± 0.2, and for a comparison discharge at q_a=4.5.

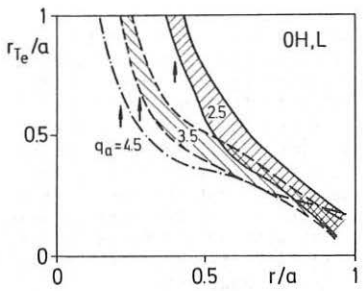

Fig.2: Radial profiles of the upper and lower bounds of the T_e scale length $r_{Te}=-T_e/dT_e/dr)$ normalized to a for the discharges used in Fig. 1 (OH, L-mode).

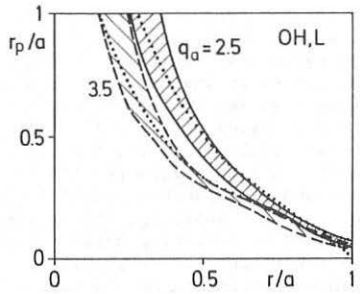

Fig.3: Radial profiles of the upper and lower bounds of the normalized presure scale length r_p/a (OH, L-mode). The dotted lines are the Kadomtsev pressure profiles with p(a)=0 for q_a=2.5 and 3.5.

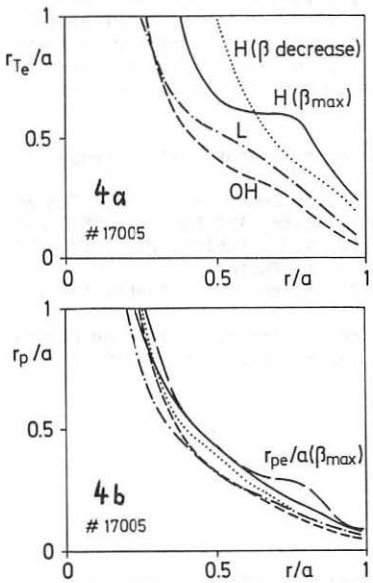

Fig.4: Radial profiles of the normalized T_e and p scale lengths for a beam heated ASDEX discharge (q_a=3.7) in different discharge phases (OH, L, H-mode).

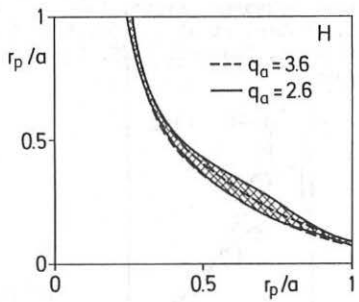

Fig.5: Radial profiles of the bounds of the normalized pressure scale length for beam-heated H mode discharges.